Acta Biomed 2019; Vol. 90, Supplement 5: 20-37 DOI: 10.23750/abm.v90i5-S.8344

Review

Internal hernias: a difficult diagnostic challenge. Review of CT signs and clinical findings

Monica Marina Lanzetta[1], Antonella Masserelli[1], Gloria Addeo[1], Diletta Cozzi[1], Nicola Maggialetti[2], Ginevra Danti[1], Lina Bartolini[1], Silvia Pradella[1], Andrea Giovagnoni[3], Vittorio Miele[1]

[1]Department of Radiology, Careggi University Hospital, Florence, Italy; [2]Department of Medicine and Health Sciences "V. Tiberio", University of Molise, Campobasso, Italy; [3] Department of Radiology, Università Politecnica delle Marche, Ancona, Italy

Summary. Although internal hernias are uncommon, they must be beared in mind in the differential diagnosis in cases of intestinal obstruction, especially in patients with no history of previous surgery or trauma. Because of the high possibility of strangulation and ischemia of the affected loops, internal hernias represent a potentially life-threatening condition and surgical emergency that needs to be quickly recognized and managed promptly. Imaging plays a leading role in the diagnosis and in particular multidetector computed tomography (MDCT), with its thin-section and high-resolution multiplanar reformatted (MPR) images, represents the first line image technique in these patients. The purpose of the present paper is to illustrate the characteristic anatomic location, the clinical findings and the CT appearance associated with main types of internal hernia, including paraduodenal, foramen of Winslow, pericecal, sigmoid-mesocolon- and trans-mesenteric- related, transomental, supravesical and pelvic hernias. (www.actabiomedica.it)

Key words: internal hernias, computed tomography, peritoneal cavity, small bowel obstruction, strangulation, mesentery, Roux -en-Y anastomosis

Introduction

An internal hernia (IH) is defined as the protrusion of abdominal viscera, most commonly small bowel loops, through a peritoneal or mesenteric aperture into a compartment in the abdominal and pelvic cavity (1-3). Cross-sectional imaging (MRI, CT and US) (4-7) techniques, gained large application in gastrointestinal radiology in the emergency department; they are is indicated as first line techniques in the diagnosis, staging and follow-up (8-23).

Hernial orifices can be congenital, including both normal foramina or recesses and unusual apertures resulting from anomalies of peritoneal attachment and internal rotation, or acquired if caused by inflammation, trauma and previous surgery, like gastric by-pass for bariatric treatment and liver transplantation. Due to the growing popularity of these surgical procedures, the overall incidence of internal hernias has been recently increasing (24). Although relatively uncommon, they represent a potentially life-threatening condition and a surgical emergency since the bowel entrapment in one of the defects can lead to acute intestinal obstruction with rapid evolution, if left untreated, into strangulation and ischemia. According to various investigators, internal hernias cause up to 5,8% of all small bowel obstruction (SBO) (3, 24-27), with a high overall mortality rate that can exceed 50% (26).

The most common manifestation of an internal hernia is strangulating SBO, that occurs after a closed-

loop obstruction (2, 11, 28, 29). However, the clinical manifestations range from mild digestive symptoms to acute abdomen, as symptom severity relates to duration and reducibility of the hernia and the presence or absence of strangulation and incarceration (24, 25, 30, 31). IHs may remain clinically silent if easily reducible, but the larger ones often cause mild discomfort ranging from constant vague epigastric pain to intermittent periumbilical pain as they occasionally show spontaneous reduction, abdominal distention, nausea and vomiting. Physical examination may reveal a palpable mass of herniated loops with localized tenderness (2, 32, 33).

This non-specific clinical presentation often leads to a delay in diagnosis, in most cases made at the time of laparotomy (3, 26), and consequently in proper treatment, carrying risk of serious complications; therefore, when the possibility of internal hernia is considered, a rapid imaging evaluation is necessary to aid an early diagnosis and a prompt intervention. Multidetector Computed Tomography (MDCT), with its wide availability, has become the first line imaging technique in these patients and play an important role in the preoperative diagnosis and planning of surgical intervention (33-37).

Classification

According to the traditional classification devised by Welch, eight main types of internal hernia can be identified on the basis of the topographic distribution of bowel loops related to the anatomic location of the orifice (38) (Fig. 1).

Despite classically paraduodenal hernia has been described as the most common type of IH, recently transmesenteric hernias have reached a higher incidence, in relation to the increasing frequency of surgical procedures in which a Roux-en-Y loop is constructed (39, 40)

Doishita et al. proposed a categorization of the various types of internal hernia in three main groups according to the type of hernia orifice, depending on whether the herniation occurs through a normal foramen, an unusual peritoneal fossa or recess into the retroperitoneum, or an abnormal opening in a mesentery or peritoneal ligament (33).

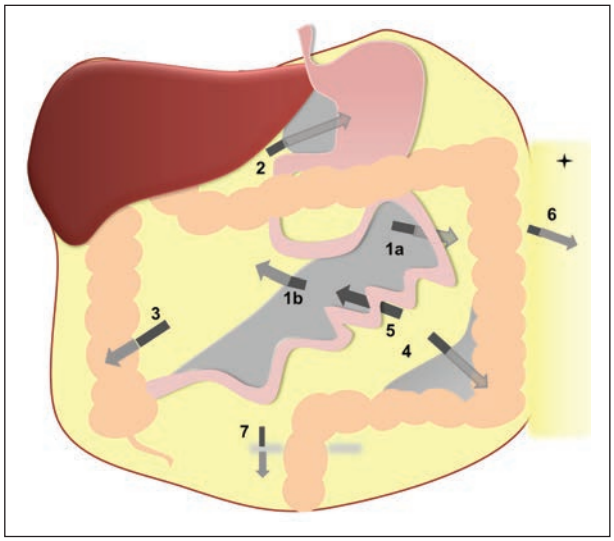

Figure 1. Drawing shows the anatomic sites of internal hernias: 1a: left paraduodenal hernia, 1b: right paraduodenal hernia, 2: foramen of Winslow hernia; 3: pericecal hernia; 4: sigmoid-mesocolon- related hernia; 5:transmesenteric hernia; 6: transomental hernia; 7:supravesical and pelvic hernia. Asterisk: greater omentum open and reflected laterally

Role of computed tomography

Since the interval between intestinal obstruction and ischemia may be short, a time-consuming diagnostic workup before surgery may be dangerous for an acutely ill patient (25, 41). CT, with its speed of execution, is the imaging modality of choice for the investigation of acute abdominal conditions (3, 42-45) and in particular is recommended for the evaluation of patients with acute SBO, particularly when clinical and initial plain film radiography indicates a higher grade obstruction or remains indeterminate e/o strangulation is suspected (46). Several studies have demonstrated the accuracy of CT in the detection of small bowel obstruction, with a sensitivity and specificity of 94-100% and 90-95% respectively (47-50). CT plays a more active role compared to conventional imaging methods in the identification of the site, level, cause of obstruction and the presence of ischemic changes at the involved bowel. Currently, with the possibility of using high quality three dimensional reformation techniques such as multiplanar reformation (MPR), maximum intensity projection (MIP) and volume rendering (VR), CT provides important advantages in

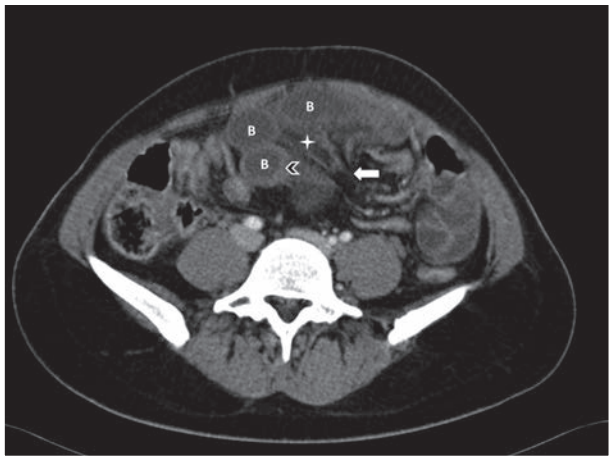

Figure 2. Closed loop small bowel obstruction. Contrast enhanced axial CT scan shows a radial array of distended small bowel loops (B) with stretched and thickened mesenteric vessels converging to a central point (white arrow). Bowel wall thickening (arrowhead) and mesenteric edema (asterisk) can also be observed.

evaluation of small bowel and surrounding structure, increasing the diagnostic confidence in the localization of the transition zone (32, 46). Small bowel obstruction of an internal hernia is usually a closed-loop obstruction, in which a segment of the bowel is occluded at two adjacent points along its course. Direct signs of a closed-loop at CT are a U- or C- shaped, fluid filled, distended intestinal loop or a radial array of distended loops with stretched and thickened mesenteric vessels converging to a central point (33, 47, 48) (Fig. 2). In this setting, a cluster of dilated loops or a 'sac-like appearance' of crowded small bowel loops owing to encapsulation within the hernia sac at an abnormal anatomic location is highly suggestive for IH (26, 33, 51). CT scans show the convergence of bowel, mesenteric fat and vessels of the closed loop in correspondence of the hernia orifice and abnormal displacement of surrounding structure and key vessels around the hernia sac (33) (Tab. 1). If intestinal strangulation is present, engorgement, twisting and dislocation of mesenteric vessels in correspondence of the hernia orifice can also be observed (46),with the detection of reduced bowel wall enhancement in cases of ischemia and pneumoperitoneum, focal discontinuity of the bowel wall and abscess or peritoneal fluid if intestinal perforation occurs (52, 53). Specific CT findings of each internal hernia are reported in table 2.

In the suspicion of IHs the use of intravenous contrast material is crucial for depicting mesenteric vessels, allowing an easier detection of hernias, and for the assessment of bowel wall vascularity. A non-enhanced scan should be obtain to detect an increased unenhanced bowel wall attenuation reflecting haemorrhagic congestion in cases of strangulation(33). A suitable CT protocol is shown in table 3.

Paraduodenal hernias (PDHs)

Background

In the classic literature paraduodenal hernias account for approximately 53% of all cases of internal hernias (3, 32). They are found more frequently in men than in women, with a ratio of 3:1, having a sex predilection unlike most types of internal hernias. There are two main subtypes: left-sided, which account for 75% of all PDHs, and right-sided, which account for the remaining 25% (32, 54, 55). Paraduodenal hernias occur when small bowel loops enter into a congenital, unusual peritoneal fossa in the vicinity of the duode-

Table 1. CT key points of internal hernias

Bowel configuration	• a saclike mass or cluster of dilated small bowel loops within an abnormal anatomic location in the setting of small bowel obstruction
Mesenteric abnormalities	• convergence of vessels and mesenteric fat at the hernia orifice • displacement of key mesenteric vessels • engorgement, crowding, twisting, stretching of mesenteric vessels if strangulation is present
Position of surrounding viscera	• displacement of surrounding structures around the hernia sac

Table 2 CT findings of internal hernia

	Bowel configuration	Mesenteric abnormalities / Anatomic landmark vessels	Effect on surrounding structures
LEFT PARADUODENAL HERNIA	encapsulated agglomerated small bowel loops with a sac-like appearance in the LUQ, lateral to the ascending duodenum, between the stomach and the pancreas, or behind the pancreatic tail, or between the transverse colon and the left adrenal gland	convergence of engorged vessels grouped together at the entrance of the hernia orifice enlargement, stretching and displacement of IMV anteriorly and leftward. IMV and left colic artery at the anterior and medial border of the hernia orifice	displacement of the posterior stomach wall anteriorly and the duodenal flessure and the transverse colon inferiorly
RIGHT PARADUODENAL HERNIA	encapsulated agglomerated small bowel loops with a sac-like appearance in the RUQ, lateral and inferior to the descending duodenum frequent association with small bowel non-rotation	convergence of engorged vessels grouped together at the entrance of the hernia orifice displacement of the SMA, right colic vein and ileocolic artery anteriorly. SMA and SMV at the anteromedial edge of the fossa the jejunal branches of SMA and SMV may be seen coursing posteriorly and to the right of the superior mesenteric vessels location of SMV to the left of and ventral to SMA if malrotation is present	rarely ureter displacement and compression
FORAMEN OF WINSLOW HERNIA	bowel loops in lesser sac between liver hilum and IVC, posterior to the stomach	convergence of engorged vessels grouped together at the entrance of the hernia orifice, elongated in front of IVC and posterior to main portal vein	displacement of the stomach antero-laterally anterior compression of main portal vein
PERICECAL HERNIA	clustered small-bowel loops with a sac-like appearance lateral to the cecum and posterior to the ascending colon in right paracolic gutter	convergence of engorged vessels grouped together at the entrance of the hernia orifice	displacement of the ascending colon anteriorly or medially
SIGMOID-MESOCOLON RELATED HERNIA	clustered small-bowel loops (with a sac-like appearance in intra e inter-mesosigmoid types) posterior and lateral to the sigmoid colon	convergence of engorged vessels grouped together at the entrance of the hernia orifice	displacement of the sigmoid colon antero-medially
TRANSMESENTERIC HERNIA	dilatated small-bowel loops, directly abutting the abdominal wall without omental fat, lateral to colon	convergence of engorged vessels grouped together at the entrance of the hernia orifice displacement of the main mesenteric trunk to the right	central displacement of the colon segments
BROAD LIGAMENT INTERNAL HERNIA	cluster of dilated small bowel loops herniated in the pelvic cavity laterally to the uterus	convergence of engorged vessels grouped together at the entrance of the hernia orifice mesenteric vessels of herniated intestine penetrating the broad ligament	displacement of the rectosigmoid dorso-laterally and of the uterus ventrally enlargement of the distance between uterus and ovary deviating in opposite directions
SUPRAVESICAL INTERNAL HERNIA	cluster of bowel loops with a sac-like appearance in front of the bladder on the left or right	crowded and engorged mesenteric vessels may be seen	compression and displacement of bladder

Table 3. CT scanning protocol

Parameter	Details
Section thickness	Preferably submillimeter (0,5-1 mm)
Interval	Same as section thickness
Scan area	Abdomen (from the xiphoid process down to the symphysis pubis)
Contrast volume	100-150 ml
Contrast flow-rate	3-4 ml/sec
Scan acquisition	• Non-enhanced scan • Arterial phase at 35-40 sec • Venous phase at 70-75 sec
Image reconstruction	• Axial 2-5 mm thickness • Multiplanar reformats in the coronal and sagittal plane at 3 mm thickness

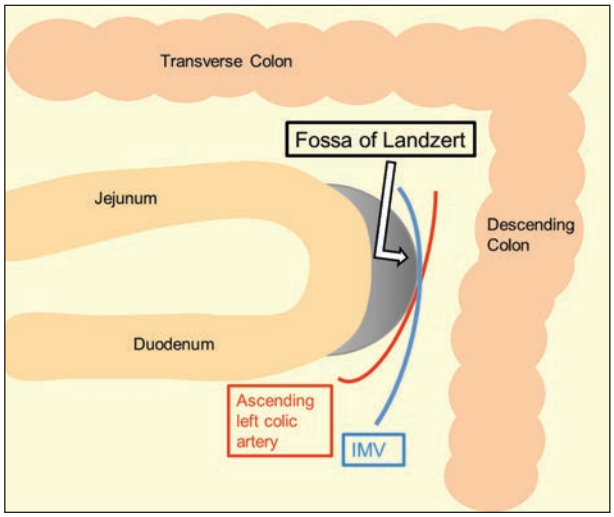

Figure 3. Graphic illustration of Landzert's fossa. The inferior mesenteric vein (IMV) and ascending left colic artery run at the anteromedial edge of the fossa

num as a result of abnormal rotation of the small intestine and failure of mesenteric fusion with the parietal peritoneum (2, 56)

Clinical findings

Patients often have a long standing history of indigestion or periodic cramps, vomiting and abdominal distention commonly dating back to the childhood; in particular postprandial pain which may be relieved by postural changes is a characteristic symptom (57). PDHs carry more than 50% lifetime risk of strangulation and intestinal infarction with a mortality rate of 20-50% (58, 59).

Left paraduodenal hernias (LPDHs)

Description

LPDHs occur when duodenal segments and jejunal loops, more often proximal, prolapse through *Landzert's fossa* (or *paraduodenal fossa*)(60), an aperture found in 2% of autopsy(32) located at the duodenojejunal junction (a zone of confluence of the descending mesocolon, transverse mesocolon and small bowel mesentery)(61), behind the descending mesocolon and to the left of the fourth part of the duodenum (33, 40). This peritoneal pocket is bordered anteriorly by a peritoneal fold lifted up by the inferior mesenteric vein (IMV) and ascending left colic artery that run at the anteromedial edge of the fossa (24, 32) (Fig. 3). In LPDHs bowel loops enter postero-inferiorly through the mesocolic defect, becoming entrapped in the Landzert's fossa, and then extend further into the descending mesocolon and the left portion of the transverse mesocolon (24, 54, 60). Since the afferent loop enters the sac from behind where the duodenum emerges from its fixed retroperitoneal position, only the efferent loop truly passes through the hernia orifice (32).

CT findings

The characteristic CT feature of LPDHs (Fig. 4) is an encapsulated cluster of commonly dilated bowel loops with a sac-like appearance in the left upper quadrant at the level of the anterior para-renal space (33). They can be noted either at the duodeno-jejunal junction between stomach and pancreas, at the level or just above and exterior to the ligament of Treitz, or behind the pancreatic tail or between transverse colon and the left adrenal gland, although these findings are non-specific (24, 60-62). Usually the herniated bowel loops cause mass effect with displacement of the posterior stomach wall anteriorly, the duodenal

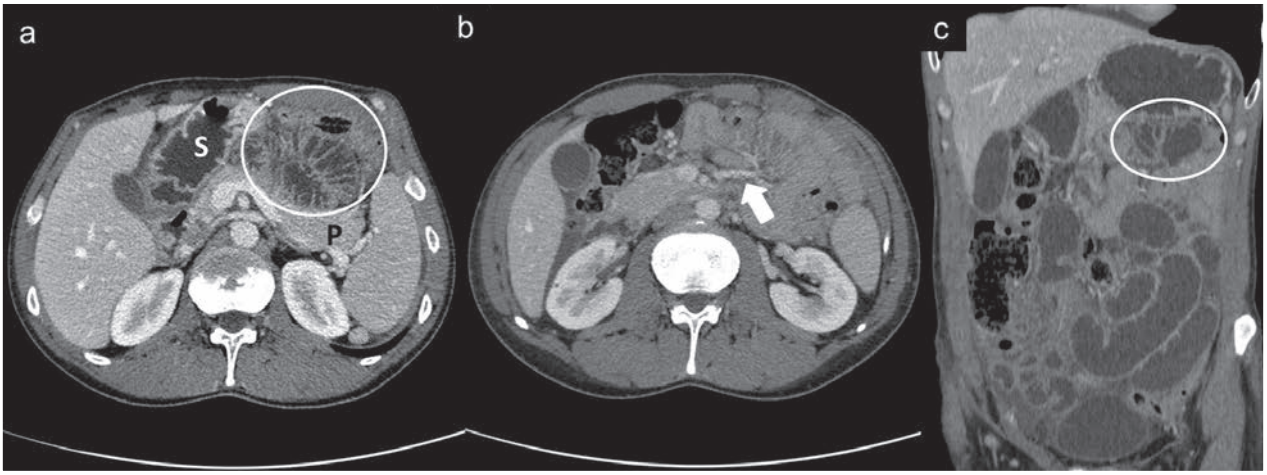

Figure 4. Left paraduodenal hernia in a 37-year-old man who presented with nausea and intense abdominal pain. Contrast-enhanced CT scans, axial (a) and (b) and coronal reformatted image (c), show a sac-like mass of clustered dilated small-bowel loops (white circles) between pancreas (P) and stomach (S) with multiple engorged and prominent vessels (white arrow) at the point of entry of the sac

flessure and the transverse colon inferiorly (1, 38, 40). CT demonstrated IMV and left colic artery as a key anatomic landmark at the anterior and medial border of the hernia orifice (33, 38). Abnormalities of the mesenteric vessel that supply the herniated loops, as crowding, stretching and enlargement at the entrance of the hernia sac as well as stretching and displacement of the IMV laterally to the left can also be observed (2, 38-40). Catalano et al. have reported a case of LPDH associated with volvulus, bowel wall ischemia and intussusception with additional CT findings like the target sign and a sausage-shaped mass composed of alternating high- and low-attenuation layers, indicative of intussusception (45, 63).

Right paraduodenal hernias (RPDHs)

Description

In RPDHs bowel's herniation occurs through the *Waldeyer's fossa* (or *mesentericoparietal fossa*), a congenital uncommon defect in the first part of the jejunal mesentery observed in no more than 1% of the population at autopsy (57). RPDHs occur most frequently in the setting of a non-rotated small intestine and a normally or incompletely rotated colon. The recess is located inferior to the third portion of duodenum, behind the root of the small bowel mesentery and extends rightward and downward into the ascending mesocolon. The superior mesenteric artery (SMA) along with the superior mesenteric vein (SMV), runs along the anteromedial edge of the fossa and represents the landmark for RPDHs (33, 61) (Fig. 5). In RPDHs the small bowel loops entrapped in this peritoneal pocket protrude through it toward the right half of the trans-

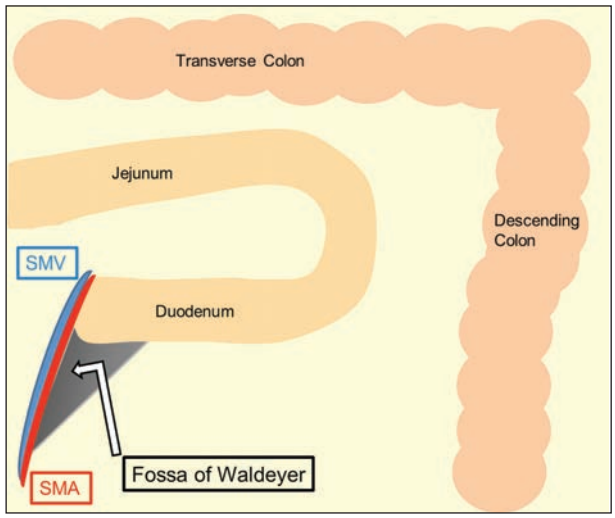

Figure 5. Graphic illustration of Waldeyer's fossa. The superior mesenteric artery (SMA) and the superior mesenteric vein (SMV) run along the anteromedial edge of the fossa

verse mesocolon behind the ascending mesocolon, lying posterior and to the right of the SMA that can be displaced anteriorly along with ileocolic artery and right colic vein, located in the anterior margin of the neck of the hernia sac (24, 38). Because both afferent and efferent loops pass through the hernia orifice where they are closely apposed and narrowed, RPDHs are usually larger and more often fixed than those occurring on the left side (32, 57).

CT findings

The characteristic CT feature of RPDHs (Fig. 6) is an encapsulated cluster of dilated small bowel loops located in the right mid abdomen, lateral and inferior to the descending duodenum (38). In addition, looping of the small intestine around the SMA and SMV at the root of the small bowel mesentery can be observed. In cases of intestinal non rotation the SMV is

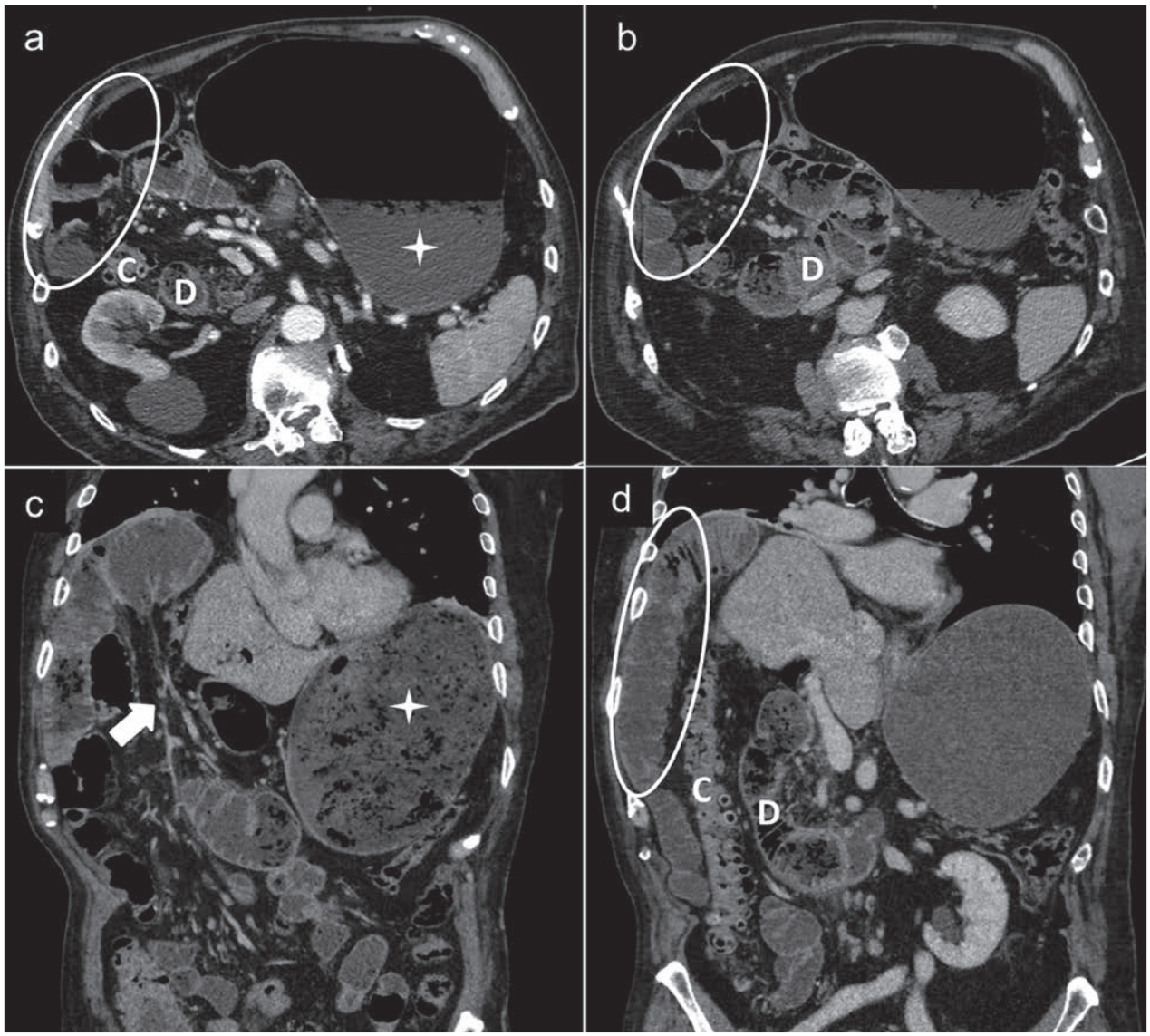

Figure 6. Right paraduodenal hernia in a 83-year-old man with mild abdominal pain and repeated episodes of vomiting for a few hours. Contrast enhanced CT scans, axial (a) and (b) and coronal reformatted image (c) and (d) show an encapsulated cluster of dilated jejunal loops in the right upper quadrant (white circles), lateral to the colon (C) and the II-III portion of duodenum (D) which appears located rightward. Gastric overdistention is also be observed (asterisks). Dilated and converging vessels (white arrow) are seen in the mesentery.

located in a more ventral and leftward position to the SMA and the horizontal duodenum is absent, with cecum in its normal position(61). Rare cases of right ureter displacement and compression have been reported, underlying the retroperitoneal location of this type of hernia (51).

Foramen of Winslow hernias (FWHs)

Background

In the classic literature FWHs constitutes 8% of all internal hernias. Foramen of Winslow hernias are the most common type of "lesser sac hernia", in which viscera enter the lesser sac (a unique remnant of the primitive right peritoneal space) through the foramen of Winslow (Fig. 7). Other types of "lesser sac hernia" include bowel herniation through abnormal aperture in only one leaf of the greater omentum or through the lesser omentum, composed of the gastrohepatic and hepatoduodenal ligaments (33). In 60%-70% of cases the herniated viscera are small bowel loops; the terminal ileum, cecum and ascending colon are involved in about 25-30%. The transverse colon, gallbladder and omentum account for the remainder (32). Several risk factors for this type of hernia have been described, including an enlarged foramen of Winslow, an usually long small bowel mesentery, common intestinal mesentery, an elongated right liver (such as Riedel lobe), persistence of the ascending mesocolon enabling increased mobility of the bowel (2, 64), a lack of fusion between cecum or ascending mesocolon to parietal peritoneum, a defect in the gastrohepatic ligament and finally an incomplete intestinal rotations or malrotations (65).

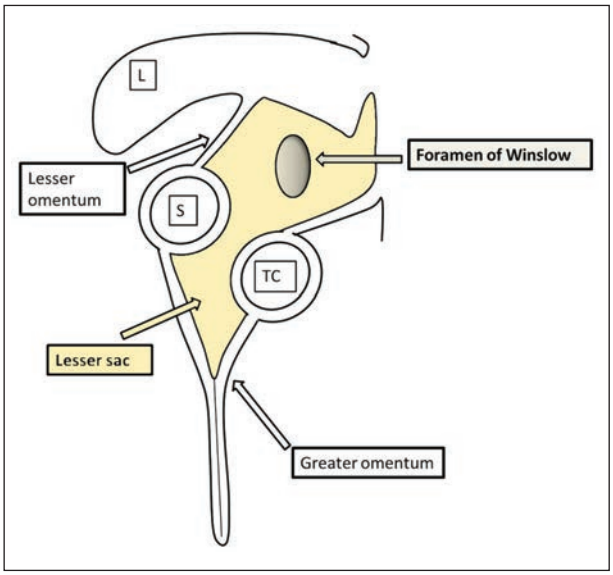

Figure 7. Graphic illustration of lesser sac and foramen of Winslow. L: liver; S:stomach; TC:transverse colon.

Clinical findings

The clinical findings of FWHs are often related to small bowel obstruction and occasionally to gastric outlet obstruction due to a compressive effect on the stomach by the herniated loops (66). Patients often present with an acute onset of a progressive abdominal pain, that can be preceded by a change in abdominal pressure, usually attenuated by forward flexion or in the position of the knee in the chest (32). An obstructive jaundice due to the compression of the hepatic pedicle by herniated gallbladder or bowel loops can also be observed, as reported by Numata et al. (67) and Welaratne et al. (68). Ye et al in 2002 have described the first case of obstructive jaundice and acute pancreatitis caused by a FWHs (69).

Since FWHs are often strangulated at presentation, they are associated with a high mortality rate of up to 49% (65).

Description

The epiploic foramen of Winslow is a congenital aperture located below the right border of the superior recess of the lesser sac, inferior to the caudate lobe of the liver, anterior to the inferior vena cava, superior to the second portion of the duodenum and posterior to the hepatoduodenal ligament (including hepatic artery, portal vein and bile duct). It represent the only communication between the greater and lesser peritoneal cavities (33).

CT findings

The characteristic CT findings of FWHs (Fig. 8) are the following: hydro-aerial levels in the lesser sac,

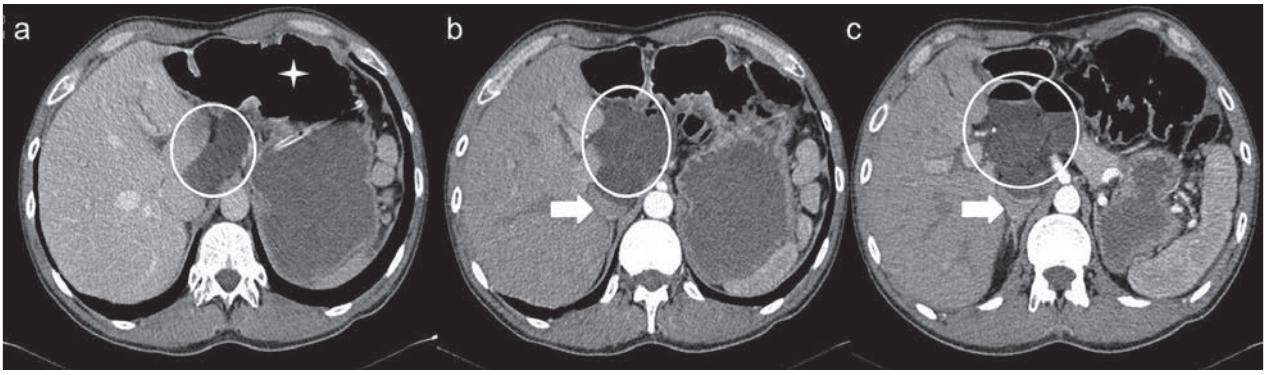

Figure 8. Foramen of Winslow hernia in a 72-year-old man with intermittent epigastric pain. Contrast-enhanced axial CT scans (a), (b) and (c) show cluster of small bowel loops located in the lesser sac (white circles) between liver and pancreas, posterior to stomach (displaced anteriorly) (asterisk) and anterior to inferior vena cava, which is compressed (white arrows)

posterior to the liver and between pancreas and stomach (which can be displaced antero-laterally) with a 'beak' directed toward the foramen of Winslow ('bird beak sign'); mesentery and associated vessels, often stretched through the foramen, located anterior to inferior vena cava and posterior to main portal vein, which can be compressed anteriorly; absence of the caecum and ascending colon in the right gutter; two or more bowel loops in the high sub hepatic space (2, 70). FWHs often presents similar radiographic features to that of left paraduodenal hernias; the absence of an encapsulated membrane is characteristic of the former, conversely a major mass effect on the transverse colon more commonly indicates a left paraduodenal hernia (24, 38).

Pericecal hernias (PCHs)

Background and Description

In the classic literature PCHs correspond of 13% of all internal hernias. Bowel loops, most commonly an ileal segment, herniate into the right paracolic gutter through a congenital or acquired (most commonly by adhesions) unusual defect in the cecal mesentery. Four different recesses in the pericecal region formed by folds of the peritoneum have been described: superior and inferior ileocecal recess, retrocecal recess and paracolic sulci (2, 33, 55). However, the diagnostic features and surgical management of the four subtypes do not differ (60).

Clinical findings

Patients commonly report recurrent episodes of colicky intense right lower abdominal pain. Chronic incarceration may produce symptoms compatible with appendiceal disordes, intestinal diseases or intestinal obstruction caused by adhesions (32). In PCHs however have been reported a higher incidence of occlusive symptoms (60) (71) with rapid progression to strangulation and a mortality rate that can be high as 75% (24, 72).

CT findings

With CT, a cluster of fixed and dilated small bowel loops with a sac-like appearance is noted, possibly extending into the right paracolic gutter, lateral to the cecum and posterior to the ascending colon, which can be displaced anteriorly or medially (2, 33, 60, 73) (Fig. 9).

Sigmoid-mesocolon related hernias (SMHs)

Background

In the classic literature SMHs account for 6% of all internal hernias. Historically Benson et al have described three many types of internal hernias involving the sigmoid mesocolon, a peritoneal fold that suspends the sigmoid colon from the posterior parietal perito-

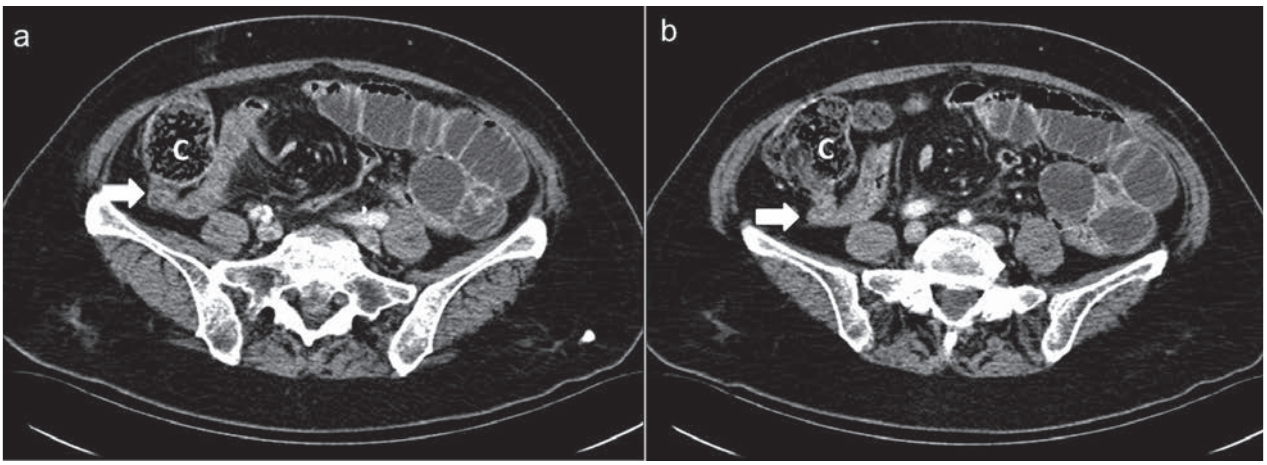

Figure 9. Pericecal hernia in a 80-year-old man with a 1- day history of right lower abdominal pain and vomiting. Contrast-enhanced axial CT scans (a) and (b) show small bowel loops (white arrows) posterior to cecum (C) in right paracolic gutter producing small bowel obstruction

neum: intersigmoid, transmesosigmoid and intramesosigmoid. The former have been reported as the most common (2, 24) (74), despite most Japanese studies have found intramesosigmoid hernias accounting for approximately half the cases (50%-57.3%), followed by intersigmoid hernia (24.5%-35%) and transmesosigmoid hernia (15%-18%)(75). These three categories are radiographically difficult to distinguish since they show similar CT findings, however not preoperative differentiation is required because surgical treatment is similar (24, 60).

Description

In the intersigmoid hernias small bowel, usually ileum, protrudes into the intersigmoid fossa, a congenital (found in 50-75% of autopsies) (74) unusual retroperitoneal recess formed between the adjacent sigmoid segments and their relative mesenteries, located above and behind the apex of the root of the sigmoid mesocolon (33, 60)In transmesosigmoid type bowel loops protrude without a hernia sac through a complete defect involving both of the peritoneal layers of the sigmoid mesentery, lying in a location lateral to the sigmoid itself. The third type, intramesosigmoid, is the herniation through only one peritoneal layer of the mesosigma (usually the left) so that the hernia sac lies within the sigmoid mesocolon (24, 60).

CT findings

CT findings in SMHs (Fig. 10) are a cluster of dilated small bowel loops entrapped posterior and lateral to the sigmoid colon, with the defect most commonly located between the sigmoid colon and the left psoas muscle, or between sigmoid loops in the intersigmoid type (24, 60, 76). In both inter- and intramesosigmoid types bowels show a sac-like appearance, absent in the transmesosigmoid type (33). Often a mass effect can be observed, with displacement of the sigmoid colon antero-medially (24, 76). Furthermore splaying of the sigmoid vessels, as if they are wrapping the hernia sac, may suggest an intramesosigmoid hernia (33, 77).

Transmesenteric and Roux-en-y anastomosis-related (TMHs) hernias

Background

A transmesenteric hernia occurs in presence of a congenital or acquired abnormal defect, involving both layers of the small bowel mesentery, usually located close the ligament of Treitz or the terminal ileum (33, 57). The small bowel mesentery is a voluminous, fat-laden peritoneal reflexion that fixes the loops of the small intestine to the posterior abdominal wall and

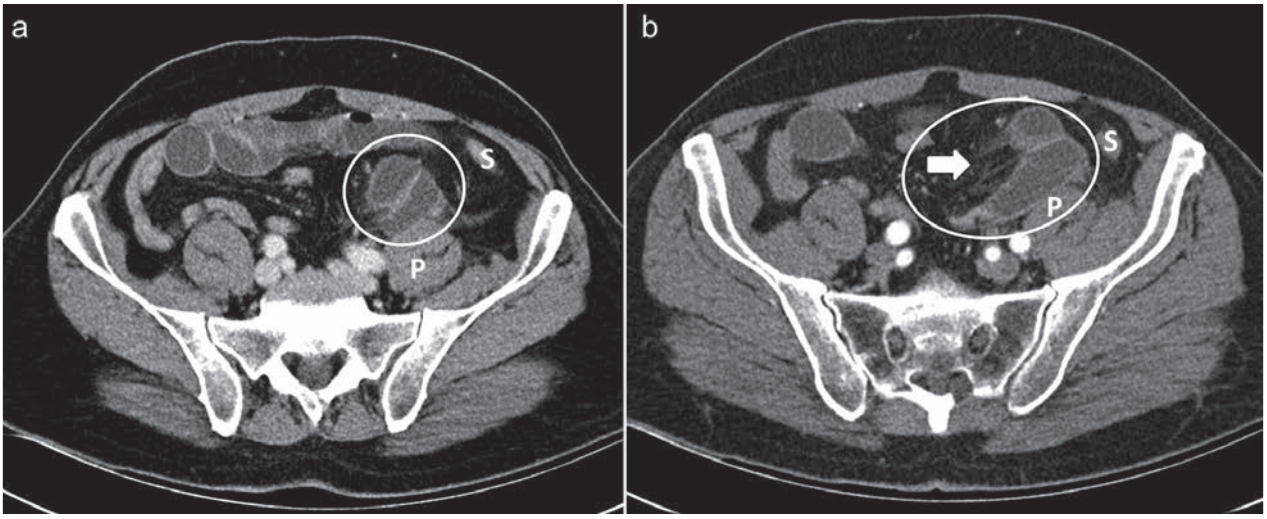

Figure 10. Sigmoid-mesocolon related hernia in a 80 year-old-man with acute left-sided abdominal pain. Contrast-enhanced axial CT scans (a) and (b) show encapsulated fluid-filled small bowel loops (white circles) protruding toward left lower abdomen through a defect in sigmoid mesocolon located near the left common iliac artery, between sigmoid colon (S) and the left psoas muscle (P). Convergence of engorged vessels grouped together at the entrance of the hernia orifice can also be seen (white arrow)

run obliquely down from its origin at the ligament of Treitz to the right toward the ileocecal junction (61). TMHs are the most common internal hernia in children. In fact almost 35% of cases occur in the pediatric age due to congenital defect in the small bowel mesentery close to the ileocecal region as a consequence of prenatal intestinal ischemia leading to thinning of the mesenteric leaves associated with bowel atresia in 5,5% of the pediatric population (78), partial regression of the dorsal mesentery, fenestration during the developmental enlargement of an inadequately vascularized area and an ileocecal mesentery with rapid and considerable lengthening in fetal life (2, 54). On the other hand, in the adult population TMHs are usually iatrogenic, being related to trauma, inflammation or previous abdominal surgery, in particular with Roux-en-Y anastomosis as in gastric by-pass or liver transplantation (2, 24, 60). In the classic literature TMHs account for approximately 8% of all internal hernias, although actually their incidence is increasing. Because of wide differences in the number of cases and follow-up time among existing research reports, the morbidity of internal hernia after laparoscopic Roux-en-Y gastric bypass fluctuates wildly between 0.2% and 9.0% (79).

Description

TMHs are difficult to detect due to the variability of their location since herniated bowel loops are not enveloped in a limiting sac and therefore can potentially be anywhere in the peritoneal cavity; however, they are detected more frequently in the right mid abdomen, usually adjacent to the abdominal wall (24, 39). Roux- en-Y anastomosis- related hernias usually occur more than one month after surgery and are more associated with the retrocolic procedure, in which the Roux limb passes through a complete defect created in the transverse mesocolon. After surgery, the defect can be incompletely closed or have a breakdown or a pulling of the suture material through the mesocolic fat; moreover enlargement of the mesenteric aperture can occur with repeated herniations or rapid weight loss and decreased peritoneal fat, common in bariatric patients, with consequent bowel herniation (24, 80-82). Furthermore, transmesenteric internal hernias in the adult postoperative patients more often occur after a laparoscopic rather than open approach because of lack of intra-abdominal adhesions required for fixation of the Roux-limb to prevent its displacement and to close mesenteric defects, as reported by Higa et al and Merkle et al. (83, 84).

Three types of Roux -en-Y related hernias have been described: '*transmesocolic*', the most common, in which bowel loops herniate through the surgical defect in the transverse mesocolon with possible mass effect on the stomach and displacement of the transverse colon anteriorly and inferiorly (24, 33); '*jejunostomy mesenteric*' if bowel prolapse through a defect in the small-bowel mesentery of the jejunojejunostomy site and finally the '*Petersen type*', in which bowel loops protrude behind the Roux loop before the small bowel eventually passes through the defect in the trasverse mesocolon in a space called Petersen defect, located between the jejunal mesentery of the Roux limb and transverse mesocolon (24, 81, 84). A deformed and displaced Roux limb, biliopancreatic limb and transverse colon may serve as landmarks of these hernias (33).

Clinical findings

Clinical findings of a TMHs often include signs of small bowel obstruction (60) with a more acute symptoms onset than other internal hernias (24, 40); vomiting is frequently absent because few secretions accumulate from the proximal gastric pouch or the Roux limb (84). A palpable abdominal mass representing "the Gordian knot of herniated intestine" may be present in a minority of patients (24). Due to the lack of delimitation which allow protrusion of a considerable length of bowel (25) and the small diameter of the mesenteric aperture (2-5 cm), transmesenteric hernias are more liable than other subtypes to develop volvulus and strangulation or ischemia, with an incidence of 30% and 40% respectively and high mortality rates reaching about of 50% for the treated groups and 100% for the non-treated groups (24, 40).

CT findings

Blachar et al. in 2001 have described the presence of clustered, compressed small bowel loops in the periphery of the abdominal cavity and the lack of omental fat between the loops and the abdominal wall as the most useful CT signs for the detection of a transmesenteric hernia. The herniated bowels appeared lateral to the colon (a reversal of the normal anatomic arrangement) with central, inferior and posterior displacement of the transverse colon and inferior and medial displacement of the hepatic flessure (40). Another study concluded that the only statistically significant CT signs predictors of a transmesenteric hernia are clustering of small bowel loops, especially those that are adjacent to the abdominal wall, mesenteric vessel abnormalities including stretching, crowding and engorgement, a displacement of the main mesenteric trunk to the right and signs of small bowel obstruction (39) (Fig. 11).

Dilauro et al. described the mesenteric swirl and small bowel obstruction as the CT signs with the highest accuracy for diagnosis of internal hernia after laparoscopic Roux-en-Y gastric bypass. The authors introduced two new signs: a 'SMV beaking' (a decreased calibre of SMV with beaked appearance), and 'criss cross appearance' of the second order mesenteric vessels with reversal of the SMV and SMA anatomic relationship (85). In literature other CT signs associated with internal mesenteric hernia following Roux-en-Y bypass gastric surgery have been described, like 'the mushroom sign' (a mushroom shaped mesenteric root between the SMA and the distal mesenteric arterial branch), the 'hurricane eye' sign (distal tubular mesentery with surrounding small bowel loops), a small bowel loop behind the SMA, abnormal position of the jejunojejunostomy, and 'weeping mesentery' (edematous mesentery with enlarged lymphnodes) (33, 85-87) (Tab. 4) (Fig. 12).

Transomental hernias (TOHs)

Background and Description

Traditionally, TOHs make up 1-4% of all IHs. The term "transomental hernia" usually refers to herniation, most commonly of small bowel loops, cecum and sigmoid colon, through or into a congenital or acquired abnormal defect of the greater omentum from 2 to 10 cm in diameter involving both leaves (four peritoneal layers) and located in the periphery near the free edge (2) .

CT findings

CT findings are often identical to those of a transmesenteric hernia, however characteristic features

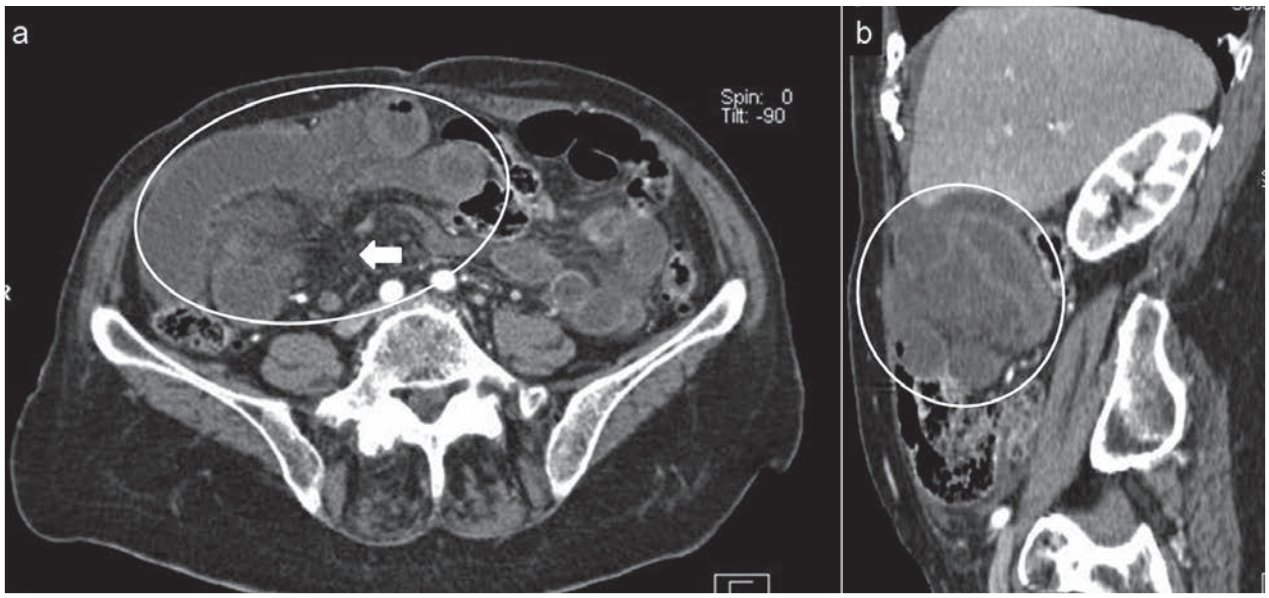

Figure 11. Transmesenteric hernia in a 28 year-old man with lower abdominal pain. Contrast-enhanced axial CT scan (a) and sagittal reformatted image (b) show distended ileal loops with poor enhancement of walls (white circles) adjacent to the right abdominal wall. The mesenteric vessels are engorged and crowded (white arrow)

Table 4. CT signs associated with Roux-en-Y anastomosis related hernia

- Swirled mesentery
- Small-bowel obstruction
- Hurricane eye
- SMV beaking
- Criss cross appearance
- Mushroom sign
- Small-bowel behind superior mesenteric artery
- Weeping mesentery
- Right-sided anastomosis

of TOHs are dilated bowel loops, without a sac-like appearance, located in the most anterior portion of the peritoneal cavity with omental vessels that run vertically around the hernia orifice (2, 24) (Fig. 13).

Supravesical and pelvic (PIHs) internal hernias

Background

Supravesical and pelvic internal hernias account for approximately 6% of all IHs. Broad ligament hernia is the most common type of pelvic internal hernias, a rare and heterogeneous group of IHs that occur in the pelvis, including also hernias through the perirectal fossa and fossa of Douglas (33). Bowel loops, usually small intestine, protrude through or into an abnormal aperture in the left or right broad ligament of the uterus, especially in multiparous middle-aged women as a consequence of developmental peritoneal defect around the uterus or acquired conditions such as pregnancy and birth trauma, injuries following vaginal manipulations or inflammatory pelvic diseases (2, 88). Herniation of colon, ovary and ureter have also been described (33, 89). Cameron et al. have reported the first case of SBO and ischemia secondary to an internal hernia due to both a defect in the broad ligament and wrapping of the fallopian tube around the bowel (90).

Description

According to the classification scheme proposed by Hunt, three categories of broad ligament hernias related to the degree of the defect have been described: '*fenestra type*', the most common, if both two peritoneal layers of the broad ligament are involved, '*pouch type*', if

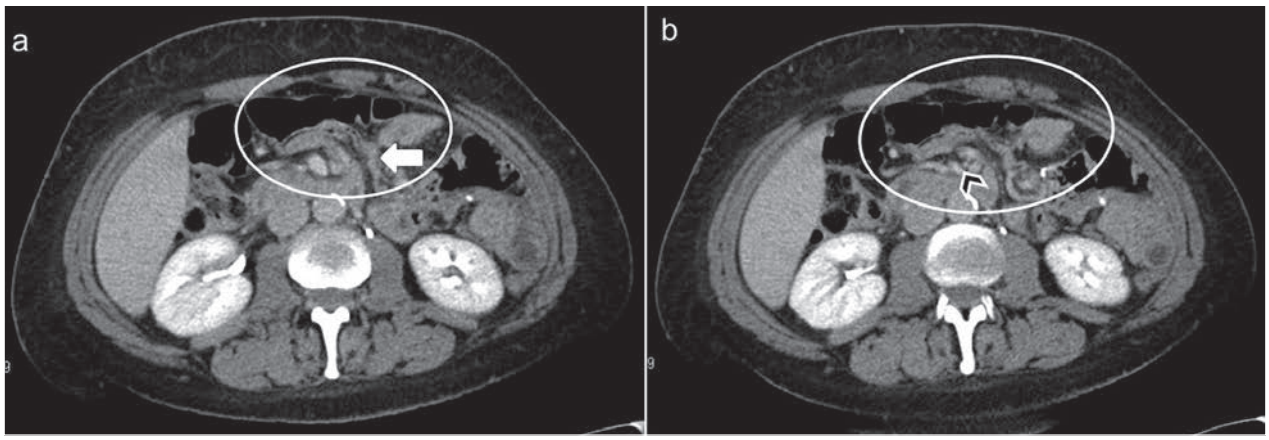

Figure 12. Petersen hernia in a 40 year-old-woman with nausea and vomiting 6 months after a Roux-en-Y gastric by-pass. Contrast-enhanced axial CT scans (a) and (b) show grouping of small bowel loops near anterior abdominal wall (white circles). A mushroom shape of the herniated mesenteric root (white arrow) and a decreased calibre of SMV with a beaked appearance are also seen (arrowhead)

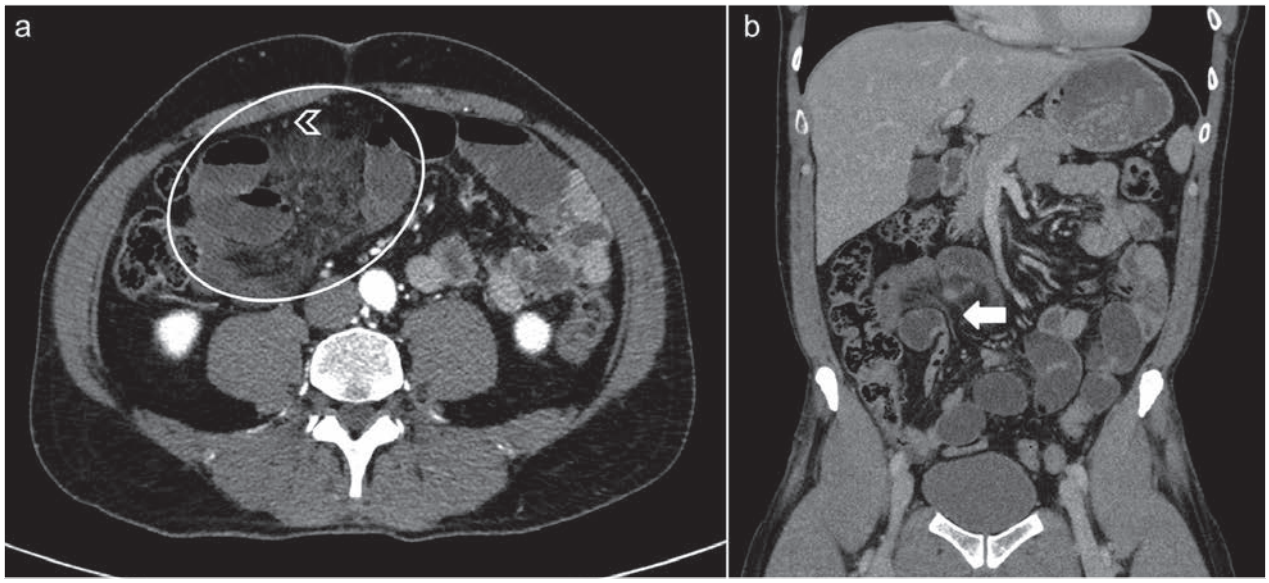

Figure 13. Transomental hernia in a 49 year-old man with diffuse abdominal pain. Contrast-enhanced axial CT scan (a) and coronal reformatted image (b) show small bowel loops (white circle) with converging mesenteric vessels and fat in the hernia orifice (white arrow). Omental vessels (arrowheads) running vertically are also seen

the defect is in only one of the two layers whereby the visceral structures would be entrapped within a sac in the parametrial tissue, and '*hernia sac type*', whereby a double layer of attenuated peritoneum lines the herniated bowel, forming a true internal hernia (88). Cilley et al. (91) introduced a new classification based on the anatomic position of the defect, which included three categories: type 1, defect caudal to the round ligament; type 2, defect above the broad ligament; and type 3, defect between the round ligament and remainder of the broad ligament, through the mesoligametum teres (88).

In internal supravesical hernias intestine protrude downward into a space around the bladder through

supravesical fossa, a triangular area bounded laterally by the left or right medial umbilical ligament, medially by the median umbilical ligament and inferiorly by the peritoneal reflection passing from the anterior abdominal wall to the dome of the urinary bladder (33, 92, 95-99). Skandalakis et al. proposed the terms "anterior supravesical", "right or left lateral supravesical", and "posterior supravesical" depending on whether the hernia passed in front of, beside or behind the bladder, respectively.

CT findings

CT findings of broad ligament hernias include a cluster of dilated small bowel loops herniated in the pelvic cavity laterally to the uterus with a displacement of the rectosigmoid dorso-laterally and of the uterus ventrally and enlargement of the distance between the uterus and the ovary deviating in opposite directions. Furthermore mesenteric vessels of herniated loops penetrating the broad ligament may be seen (33, 88). In supravesical internal hernia usually CT scans show bowel loops with a sac-like appearance pass into the space of Retzius and lay in front of the compressed bladder on the left or right. These patients can present with bladder irritation and dysuria, as the bladder is compressed by the small bowel (33, 93, 94) (Fig. 14).

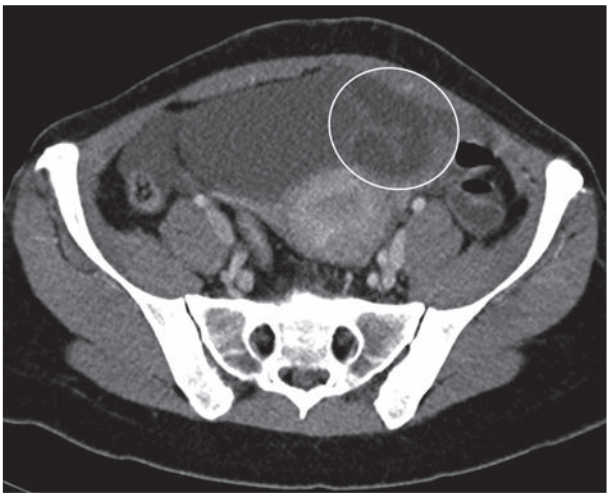

Figure 14. Internal supravesical hernia in a 67-year-old woman with a two-day history of lower abdominal pain. Contrast-enhanced axial CT scan shows intestine loops (white circle) to the left of the urinary bladder.

Conclusions

Although internal hernias are uncommon conditions, they must be considered in the differential diagnosis of acute abdominal pain, especially in presence of strangulated closed loop small bowel obstruction without external hernias or history of previous surgery or trauma and in gastric bypass patients. In the acute setting a prompt imaging diagnosis is mandatory in order to avoid intestinal ischemia and necrosis. Radiologists play a key role in detection of internal hernias and it is very important for them to be familiarized with the anatomy, aetiology and CT signs of these hernias to aid an accurate and quickly preoperative diagnosis and improve patient's outcome guiding surgeons to ensure the appropriate management in order to reduce morbidity and mortality rates.

Ethical approval: This article does not contain any studies with human participants performed by any of the authors.

Conflict of interest: None to declare

References

1. Miller PA, Mezwa DG, Feczko PJ, Jafri ZH, Madrazo BL. Imaging of abdominal hernias. Radiographics 1995; 15: 333-47.
2. Takeyama N, Gokan T, Ohgiya Y, et al. CT of internal hernias. Radiographics 2005; 25: 997-1015.
3. Akyildiz H, Artis T, Sozuer E, et al. Internal hernia: complex diagnostic and therapeutic problem. Int J Surg 2009; 7: 334-7.
4. Caranci F, Napoli M, Cirillo M, Briganti G, Brunese L, Briganti F. Basilar artery hypoplasia. Neuroradiol J 2012; 25: 739-43.
5. Cirillo M, Caranci F, Tortora F, et al. Structural neuroimaging in dementia. J Alzheimers Dis 2012; 29: 16-19.
6. di Giacomo V, Trinci M, van der Byl G, Catania VD, Calisti A, Miele V. Ultrasound in newborns and children suffering from non-traumatic acute abdominal pain: imaging with clinical and surgical correlation. J Ultrasound 2015; 18: 385-93.
7. Iacobellis F, Segreto T, Berritto D, et al. A rat model of acute kidney injury through systemic hypoperfusion evaluated by micro-US, color and PW-Doppler. Radiol Med 2018;
8. Barile A, Bruno F, Arrigoni F, et al. Emergency and Trauma of the Ankle. Semi Musc Rad 2017; 21: 282-89.
9. Barile A, Bruno F, Mariani S, et al. What can be seen after rotator cuff repair: a brief review of diagnostic imaging findings. Musculoskelet Surg 2017; 101: 3-14.

10. Cantisani V, Grazhdani H, Drakonaki E, et al. Strain US elastography for the characterization of thyroid nodules: Advantages and limitation. Int J Endocrinol 2015; 2015:
11. Mandato Y, Reginelli A, Galasso R, Iacobellis F, Berritto D, Cappabianca S. Errors in the Radiological Evaluation of the Alimentary Tract: Part I. Semin Ultrasound CT MR 2012; 33: 300-07.
12. Gatta G, Parlato V, Di Grezia G, et al. Ultrasound-guided aspiration and ethanol sclerotherapy for treating endometrial cysts. Radiol Med 2010; 115: 1330-39.
13. Scialpi M, Cappabianca S, Rotondo A, et al. Pulmonary congenital cystic disease in adults. Spiral computed tomography findings with pathologic correlation and management. Radiol Med 2010; 115: 539-50.
14. Sverzellati N, Calabrò E, Chetta A, et al. Visual score and quantitative CT indices in pulmonary fibrosis: Relationship with physiologic impairment. Radiol Med 2007; 112: 1160-72.
15. Vivarelli M, Vincenzi P, Montalti R, et al. ALPPS Procedure for Extended Liver Resections: A Single Centre Experience and a Systematic Review. PLoS One 2015; 10: e0144019.
16. Valeri G, Mazza FA, Maggi S, et al. Open source software in a practical approach for post processing of radiologic images. Radiol Med 2015; 120: 309-23.
17. Mocchegiani F, Vincenzi P, Coletta M, et al. Prevalence and clinical outcome of hepatic haemangioma with specific reference to the risk of rupture: A large retrospective cross-sectional study. Dig Liver Dis 2016; 48: 309-14.
18. Schicchi N, Valeri G, Moroncini G, et al. Myocardial perfusion defects in scleroderma detected by contrast-enhanced cardiovascular magnetic resonance. Radiol Med 2014; 119: 885-94.
19. Tarantini G, Favaretto E, Napodano M, et al. Design and methodologies of the postconditioning during coronary angioplasty in acute myocardial infarction (POST-AMI) trial. Cardiology 2010; 116: 110-16.
20. Salvolini L, Urbinati C, Valeri G, Ferrara C, Giovagnoni A. Contrast-enhanced MR cholangiography (MRCP) with GD-EOB-DTPA in evaluating biliary complications after surgery. Radiol Med 2012; 117: 354-68.
21. Sforza V, Martinelli E, Ciardiello F, et al. Mechanisms of resistance to anti-epidermal growth factor receptor inhibitors in metastatic colorectal cancer. World J Gastroenterol 2016; 22: 6345-61.
22. Maurizi N, Passantino S, Spaziani G, et al. Long-term Outcomes of Pediatric-Onset Hypertrophic Cardiomyopathy and Age-Specific Risk Factors for Lethal Arrhythmic Events. JAMA Cardiol 2018; 3: 520-25.
23. Di Pietto F, Chianca V, de Ritis R, et al. Postoperative imaging in arthroscopic hip surgery. Musculoskelet Surg 2017; 101: 43-49.
24. Martin LC, Merkle EM, Thompson WM. Review of internal hernias: radiographic and clinical findings. AJR Am J Roentgenol 2006; 186: 703-17.
25. Fan HP, Yang AD, Chang YJ, Juan CW, Wu HP. Clinical spectrum of internal hernia: a surgical emergency. Surg Today 2008; 38: 899-904.
26. Kar S, Mohapatra V, Rath PK. A Rare Type of Primary Internal Hernia Causing Small Intestinal Obstruction. Case Rep Surg 2016; 2016: 3540794.
27. Fujiwara T, Ohno Y, Sasaki A, Suzaki N, Matsuo Y. Internal hernia with triple hiatus of congenital origin: report of a case. Surg Today 2000; 30: 954-8.
28. Reginelli A, Mandato Y, Solazzo A, Berritto D, Iacobellis F, Grassi R. Errors in the Radiological Evaluation of the Alimentary Tract: Part II. Semin Ultrasound CT MR 2012; 33: 308-17.
29. Cappabianca S, Reginelli A, Monaco L, Del Vecchio L, Di Martino N, Grassi R. Combined videofluoroscopy and manometry in the diagnosis of oropharyngeal dysphagia: Examination technique and preliminary experience. Radiol Med 2008; 113: 923-40.
30. Blachar A, Federle MP. Internal hernia: an increasingly common cause of small bowel obstruction. Semin Ultrasound CT MR 2002; 23: 174-83.
31. Dionigi G, Dionigi R, Rovera F, et al. Treatment of high output entero-cutaneous fistulae associated with large abdominal wall defects: single center experience. Int J Surg 2008; 6: 51-6.
32. Gore RM, Levine MS, Textbook of Gastrointestinal Radiology E-Book, Elsevier Health Sciences2014.
33. Doishita S, Takeshita T, Uchima Y, et al. Internal Hernias in the Era of Multidetector CT: Correlation of Imaging and Surgical Findings. Radiographics 2016; 36: 88-106.
34. Maggialetti N, Capasso R, Pinto D, et al. Diagnostic value of computed tomography colonography (CTC) after incomplete optical colonoscopy. Int J Surg 2016; 33 Suppl 1: S36-44.
35. Di Cesare E, Patriarca L, Panebianco L, et al. Coronary computed tomography angiography in the evaluation of intermediate risk asymptomatic individuals. Radiol Med 2018; 123: 686-94.
36. Pradella S, Lucarini S, Colagrande S. Liver lesion characterization: The wrong choice of contrast agent can mislead the diagnosis of hemangioma. Am J Roentgenol 2012; 199:
37. Di Cesare E, Gennarelli A, Di Sibio A, et al. Assessment of dose exposure and image quality in coronary angiography performed by 640-slice CT: a comparison between adaptive iterative and filtered back-projection algorithm by propensity analysis. Radiol Med 2014; 119: 642-49.
38. Murali Appavoo Reddy UD, Dev B, Santosham R. Internal hernias: surgeons dilemma-unravelled by imaging. Indian J Surg 2014; 76: 323-8.
39. Blachar A, Federle MP, Brancatelli G, Peterson MS, Oliver JH, 3rd, Li W. Radiologist performance in the diagnosis of internal hernia by using specific CT findings with emphasis on transmesenteric hernia. Radiology 2001; 221: 422-8.
40. Blachar A, Federle MP, Dodson SF. Internal hernia: clinical and imaging findings in 17 patients with emphasis on CT criteria. Radiology 2001; 218: 68-74.

41. McDonagh T, Jelinek GA. Two cases of paraduodenal hernia, a rare internal hernia. J Accid Emerg Med 1996; 13: 64-8.
42. Regine G, Stasolla A, Miele V. Multidetector computed tomography of the renal arteries in vascular emergencies. Eur J Radiol 2007; 64: 83-91.
43. De Cecco CN, Buffa V, Fedeli S, et al. Preliminary experience with abdominal dual-energy CT (DECT): True versus virtual nonenhanced images of the liver. Radiol Med 2010; 115: 1258-66.
44. Buffa V, Solazzo A, D'Auria V, et al. Dual-source dual-energy CT: dose reduction after endovascular abdominal aortic aneurysm repair. Radiol Med 2014; 119: 934-41.
45. Valentini V, Buquicchio GL, Galluzzo M, et al. Intussusception in Adults: The Role of MDCT in the Identification of the Site and Cause of Obstruction. Gastroenterol Res Pract 2016; 2016: 5623718.
46. Zaiton F, Al-Azzazy MZ, Ahmed AS, Amr WM. MDCT signs predicting internal hernia and strangulation in patients presented to emergency department with acute small bowel obstruction. The Egyptian Journal of Radiology and Nuclear Medicine 2016; 47: 1185-94.
47. Boudiaf M, Soyer P, Terem C, Pelage JP, Maissiat E, Rymer R. Ct evaluation of small bowel obstruction. Radiographics 2001; 21: 613-24.
48. Pothiawala S, Gogna A. Early diagnosis of bowel obstruction and strangulation by computed tomography in emergency department. World J Emerg Med 2012; 3: 227-31.
49. Rosen MP, Siewert B, Sands DZ, Bromberg R, Edlow J, Raptopoulos V. Value of abdominal CT in the emergency department for patients with abdominal pain. Eur Radiol 2003; 13: 418-24.
50. Yaghmai V, Nikolaidis P, Hammond NA, Petrovic B, Gore RM, Miller FH. Multidetector-row computed tomography diagnosis of small bowel obstruction: can coronal reformations replace axial images? Emerg Radiol 2006; 13: 69-72.
51. Harbin WP. Computed tomographic diagnosis of internal hernia. Radiology 1982; 143: 736.
52. Pinto A, Miele V, Schilliro ML, et al. Spectrum of Signs of Pneumoperitoneum. Semin Ultrasound CT MR 2016; 37: 3-9.
53. Sessa B, Galluzzo M, Ianniello S, Pinto A, Trinci M, Miele V. Acute Perforated Diverticulitis: Assessment With Multidetector Computed Tomography. Semin Ultrasound CT MR 2016; 37: 37-48.
54. Shadhu K, Ramlagun D, Ping X. Para-duodenal hernia: a report of five cases and review of literature. BMC Surg 2018; 18: 32.
55. Selcuk D, Kantarci F, Ogut G, Korman U. Radiological evaluation of internal abdominal hernias. Turk J Gastroenterol 2005; 16: 57-64.
56. Zenitani M, Sasaki T, Tanaka N, Oue T. Strangulated right paraduodenal hernia successfully treated with single-incision transumbilical surgery. J Pediatr Surg Case Rep 2017; 22: 1-4.
57. Morton A. Meyers MDFF, Chusilp Charnsangavej MDF, Michael Oliphant MDF, Meyers' Dynamic Radiology of the Abdomen: Normal and Pathologic Anatomy, Springer New York2010.
58. Gusz JR, Wright LM. Intestinal obstruction secondary to left paraduodenal hernia. J Surg Case Rep 2015; 2015:
59. Barbosa L, Ferreira A, Povoa AA, Maciel JP. Left paraduodenal hernia: a rare cause of small bowel obstruction in the elderly. BMJ Case Rep 2016; 2016:
60. Mathieu D, Luciani A, Group G. Internal abdominal herniations. AJR Am J Roentgenol 2004; 183: 397-404.
61. Okino Y, Kiyosue H, Mori H, et al. Root of the small-bowel mesentery: correlative anatomy and CT features of pathologic conditions. Radiographics 2001; 21: 1475-90.
62. Suchato C, Pekanan P, Panjapiyakul C. CT findings in symptomatic left paraduodenal hernia. Abdom Imaging 1996; 21: 148-9.
63. Catalano OA, Bencivenga A, Abbate M, Tomei E, Napolitano M, Vanzulli A. Internal hernia with volvulus and intussusception: case report. Abdom Imaging 2004; 29: 164-5.
64. Erskine JM. Hernia through the foramen of Winslow. Surg Gynecol Obstet 1967; 125: 1093-109.
65. Sikiminywa-Kambale P, Anaye A, Roulet D, Pezzetta E. Internal hernia through the foramen of Winslow: a diagnosis to consider in moderate epigastric pain. J Surg Case Rep 2014; 2014:
66. Leung E, Bramhall S, Kumar P, Mourad M, Ahmed A. Internal Herniation Through Foramen of Winslow: A Diagnosis Not to Be Missed. Clinical medicine insights. Gastroenterology 2016; 9: 31-33.
67. Numata K, Kunishi Y, Kurakami Y, et al. Gallbladder herniation into the lesser sac through the foramen of Winslow: report of a case. Surg Today 2013; 43: 1194-8.
68. Welaratne I, Nasoodi A. A Rare Cause of Obstructive Jaundice: Cecal Herniation through the Foramen of Winslow. J Clin Imaging Sci 2018; 8: 24.
69. Joo YE, Kim HS, Choi SK, et al. Internal hernia presenting as obstructive jaundice and acute pancreatitis. Scand J Gastroenterol 2002; 37: 983-6.
70. Schuster MR, Tu RK, Scanlan KA. Caecal herniation through the foramen of Winslow: diagnosis by computed tomography. Br J Radiol 1992; 65: 1047-48.
71. Gullino D, Giordano O, Gullino E. [Internal hernia of the abdomen. Apropos of 14 cases]. J Chir (Paris) 1993; 130: 179-95.
72. Kleyman S, Ashraf S, Daniel S, Ananthan D, Sanni A, Khan F. Pericecal hernia: a rare form of internal hernias. J Surg Case Rep 2013; 2013:
73. Fu CY, Chang WC, Lu HE, Su CJ, Tan KH. Pericecal hernia of the inferior ileocecal recess: CT findings. Abdom Imaging 2007; 32: 81-3.
74. Benson JR, Killen DA. Internal Hernias Involving the Sigmoid Mesocolon. Ann Surg 1964; 159: 382-4.
75. Kayano H, Nomura E, Kuramoto T, et al. Two Cases of Laparoscopic Diagnosis and Treatment of Intersigmoid Hernia. Tokai J Exp Clin Med 2017; 42: 109-14.
76. Yu CY, Lin CC, Yu JC, Liu CH, Shyu RY, Chen CY. Stran-

gulated transmesosigmoid hernia: CT diagnosis. Abdom Imaging 2004; 29: 158-60.
77. Takeshita T, Ninoi T, Shigeoka H, Hirayama Y, Miki Y. Small bowel obstruction due to an intramesosigmoid hernia diagnosed by multidetector row computed tomography: a case report. Osaka city medical journal 2011; 56: 37-45.
78. Elmadi A, Lechqar M, El Biache I, et al. Trans-mesenteric hernia in infants: report of two cases. J Neonatal Surg 2014; 3: 29.
79. Farukhi MA, Mattingly MS, Clapp B, Tyroch AH. CT Scan Reliability in Detecting Internal Hernia after Gastric Bypass. JSLS 2017; 21: e2017.00054.
80. Blachar A, Federle MP. Bowel obstruction following liver transplantation: clinical and ct findings in 48 cases with emphasis on internal hernia. Radiology 2001; 218: 384-8.
81. Blachar A, Federle MP, Pealer KM, Ikramuddin S, Schauer PR. Gastrointestinal complications of laparoscopic Roux-en-Y gastric bypass surgery: clinical and imaging findings. Radiology 2002; 223: 625-32.
82. Filip JE, Mattar SG, Bowers SP, Smith CD. Internal hernia formation after laparoscopic Roux-en-Y gastric bypass for morbid obesity. Am Surg 2002; 68: 640-3.
83. Higa KD, Ho T, Boone KB. Internal hernias after laparoscopic Roux-en-Y gastric bypass: incidence, treatment and prevention. Obes Surg 2003; 13: 350-4.
84. Merkle EM, Hallowell PT, Crouse C, Nakamoto DA, Stellato TA. Roux-en-Y gastric bypass for clinically severe obesity: normal appearance and spectrum of complications at imaging. Radiology 2005; 234: 674-83.
85. Dilauro M, McInnes MD, Schieda N, et al. Internal Hernia after Laparoscopic Roux-en-Y Gastric Bypass: Optimal CT Signs for Diagnosis and Clinical Decision Making. Radiology 2017; 282: 752-60.
86. Lockhart ME, Tessler FN, Canon CL, et al. Internal hernia after gastric bypass: sensitivity and specificity of seven CT signs with surgical correlation and controls. AJR Am J Roentgenol 2007; 188: 745-50.
87. Iannuccilli JD, Grand D, Murphy BL, Evangelista P, Roye GD, Mayo-Smith W. Sensitivity and specificity of eight CT signs in the preoperative diagnosis of internal mesenteric hernia following Roux-en-Y gastric bypass surgery. Clin Radiol 2009; 64: 373-80.
88. Matsunami M, Kusanagi H, Hayashi K, Yamada S, Kano N. Broad ligament hernia successfully treated by laparoscopy: Case report and review of literature. Asian J Endosc Surg 2014; 7: 327-9.
89. Quiroga S, Sarrias M, Sanchez JL, Rivero J. Small bowel obstruction secondary to internal hernia through a defect of the broad ligament: preoperative multi-detector CT diagnosis. Abdom Imaging 2012; 37: 1089-91.
90. Cameron M, Janakan G, Birch D, Nazir S. A closed loop obstruction caused by entrapment of the fallopian tube and herniation through the broad ligament. Int J Surg 2015; 12: 57-59.
91. Cilley R, Poterack K, Lemmer J, Dafoe D. Defects of the broad ligament of the uterus. Am J Gastroenterol 1986; 81: 389-91.
92. Jan YT, Jeng KS, Liu YP, Yang FS. Internal supravesical hernia. Am J Surg 2008; 196: e27-8.
93. Morimoto M, Honjo S, Sakamoto T, et al. Internal supravesical hernia repaired via the anterior approach alone: A case report. Int J Surg Case Rep 2017; 39: 297-300.
94. Cisse M, Konate I, Ka O, Dieng M, Dia A, Toure CT. Internal supravesical hernia as a rare cauase of intestinal obstruction: a case report. J Med Case Rep 2009; 3: 9333.
95. Gafà G, Sverzellati N, Bonati E, et al (2012). Follow-up in pulmonary sarcoidosis: comparison between HRCT and pulmonary function tests. RAD. MED, vol. 117, p. 968-978, ISSN: 0033-8362, doi: 10.1007/s11547-012-0827-5
96. Bertolini L, Vaglio A, Bignardi L, et al (2011). Subclinical interstitial lung abnormalities in stable renal allograft recipients in the era of modern immunosuppression. Transplantation Proceedings, vol. 43, p. 2617-2623, ISSN: 0041-1345, doi: 10.1016/j.transproceed.2011.06.033
97. Palma BD, Guasco D, Pedrazzoni M, et al. Osteolytic lesions, cytogenetic features and bone marrow levels of cytokines and chemokines in multiple myeloma patients: Role of chemokine (C-C motif) ligand20. Leukemia. 2016 Feb;30(2):409-16. doi: 10.1038/leu.2015.259. Epub 2015 Sep 30.
98. Bozzetti C, Nizzoli R, Tiseo M, et al. ALK and ROS1 rearrangements tested by fluorescence in situ hybridization in cytological smears from advanced non-small cell lung cancer patients. Diagnostic Cytopathology, vol. 43, p. 941-946, ISSN: 8755-1039, doi: 10.1002/dc.23318
99. De Filippo M, Onniboni M, Rusca M, et al. (2008). Advantages of multidetector row CT with multiplanar reformation in guiding percutaneous lung biopsies. RAD. MED, vol. 113, p. 945-953, ISSN: 0033-8362, doi: 10.1007/s11547-008-0325-y

Received: 26 March 2019
Accepted: 4 April 2019
Correspondence:
Silvia Pradella
Department of Radiology – Careggi University Hospital
L.go G.A. Brambilla, 3 - 50134 Florence, Italy
E-mail: pradella3@yahoo.it